International Journal of Modern Physics E
Vol. 17, Supplement (2008) 8–20

World Scientific
www.worldscientific.com

FIRST RESULTS WITH THE RISING ACTIVE STOPPER*

P. H. REGAN†, N. ALKHOMASHI, N. AL-DAHAN, Zs. PODOLYÁK, S. B. PIETRI‡, S. J. STEER, A. B. GARNSWORTHY§, E. B. SUCKLING, P. D. STEVENSON, G. FARRELLY, I. J. CULLEN, W. GELLETLY and P. M. WALKER

Department of Physics, University of Surrey, Guildford, GU2 7XH, UK
†*p.regan@surrey.ac.uk*

J. BENLLIURE, A. I. MORALES, E. CASAJEROS and M. E. ESTEVEZ

Universidad de Santiago de Compostela, E-15706, Santiago de Compostela, Spain

J. GERL, M. GÓRSKA, H. J. WOLLERSHEIM, P. BOUTACHKOV, S. TASHENOV, I. KOJOUHAROV, H. SCHAFFNER, N. KURZ and R. KUMAR¶

GSI, Planckstrasse 1, D-64291, Darmstadt, Germany

B. RUBIO, A. ALGORA‖ and F. MOLINA

Instituto de Fisica Corpuscular, Universidad de Valencia, E-46071, Spain

J. GREBOSZ

The Henryk Niewodniczanski Institute of Nuclear Physics, PL-31-342, Krakow, Poland

G. BENZONI

INFN, Universitá degli Studi di Milano, I-20133, Milano, Italy

D. MÜCHER

IKP, Universität zu Köln, D-50937, Köln, Germany

A. M. BRUCE, A. M. DENIS BACELAR and S. LALKOVSKI

School of Environment and Technology, University of Brighton, Brighton, BN2 4GJ, UK

*This work is supported by the EPSRC and STFC(UK), the EU Access to Large Scale Facilities Programme (EURONS, EU contract 506065), The Spanish Ministerio de Educacion y Ciencia and The German BMBF.
†Corresponding author.
‡Present address, GSI, Planckstrasse 1, D-64291, Darmstadt, Germany.
§Current address, TRIUMF, 4004 Wesbrook Mall, Vancouver, BC V6T 2A3, Canada.
¶On leave from Inter University Accelerator Centre, New Delhi, India.
‖On leave from MTA ATOMKI, Debrecen, Hungary.

Y. FUJITA
Department of Physics, Osaka University Toyonaka, Osaka 560–0043, Japan

A. TAMII
Reseach Center for Nuclear Physics, Osaka University, Ibaraki, Osaka 567-0047, Japan

R. HOISCHEN
Department of Physics, Lund University, Lund, S-22100 Lund, Sweden

Z. LIU and P. J. WOODS
Department of Physics and Astronomy, University of Edinburgh, Edinburgh, UK

C. MIHAI
National Institute for Physics and Nuclear Engineering, RO-077125, Bucharest, Romania

J. J. VALIENTE-DOBÓN
INFN-Laboratori Nazionali di Legnaro, Italy

This paper outlines some of the physics opportunities available with the GSI RISING active stopper and presents preliminary results from an experiment aimed at performing beta-delayed gamma-ray spectroscopic studies in heavy-neutron-rich nuclei produced following the projectile fragmentation of a 1 GeV per nucleon ^{208}Pb primary beam. The energy response of the silicon active stopping detector for both heavy secondary fragments and beta-particles is demonstrated and preliminary results on the decays of neutron-rich Tantalum (Ta) to Tungsten (W) isotopes are presented as examples of the potential of this technique to allow new structural studies in hitherto experimentally unreachable heavy, neutron-rich nuclei. The resulting spectral information inferred from excited states in the tungsten daughter nuclei are compared with results from axially symmetric Hartree–Fock calculations of the nuclear shape and suggest a change in ground state structure for the N = 116 isotone ^{190}W compared to the lighter isotopes of this element.

1. Introduction

The structure of nuclei with exotic proton-to-neutron ratios is at the forefront of current nuclear physics research. In particular, the use of high-energy beams of radioactive nuclei produced following relativistic projectile fragmentation and/or fission reactions allows the production and synthesis of hitherto unreachable nuclei in the outer regions of the Segré chart.[1]

By utilizing magnetic separators such as the Fragment Separator (FRS) at GSI,[2] specific nuclei of interest can be distinguished from the vast plethora of other secondary products from such reactions and cleanly transmitted to a final focus, where spectral studies may be performed. Such studies using gamma-ray spectroscopy include decays from isomeric states in exotic nuclei[3–13] and/or (b) decay studies following alpha and/or beta-decay of the exotic nucleus.

This paper focusses on the first results using the Stopped RISING Active Stopper which allows correlations to be made between the exotic heavy-ions produced by

relativistic fragmentation/fission reactions and their subsequent beta-decays. This in turn allows beta-delayed spectroscopy to be performed in the daughter nucleus, representing, in some cases, the first spectral information in such systems.

2. The Stopped RISING Gamma-Ray Setup

The RISING gamma-ray array[14] consists of fifteen, high efficiency seven-element germanium cluster detectors. These detectors can be placed in a number of different geometries to allow inter-alia studies of "fast" fragmentation beams[15] and decay studies[16,17] using a close, compact set-up. The latter represents the "Stopped RISING" set-up[10,11,13,16,17] which is the focus of the current paper. In the Stopped-Beam configuration, the RISING detectors are placed in three rings of 5 cluster-detectors, providing a photo-peak efficiency for decay studies using fragmentation beams of ∼15% at 662 keV.[16,17]

2.1. *The RISING active stopper*

Figure 1 shows a schematic of the experimental set-up for the active stopper measurements using the RISING gamma-ray array.

The RISING Active Stopper consists of a series of Double Sided Silicon Strip Detectors (DSSSDs) and is made up of (up to) 6 DSSSDs, each with 16 horizontal and vertical strips respectively, giving 256 pixels per DSSSD. Each DSSSD was 5 cm by 5 cm in overall dimension and 1 mm thick. The DSSSDs were used to determine both the energy and position of the (a) implanted secondary fragment of interest directly from the projectile fragmentation reaction and (b) beta-particle(s) following the subsequent radioactive decay(s) of the often highly exotic nucleus of interest

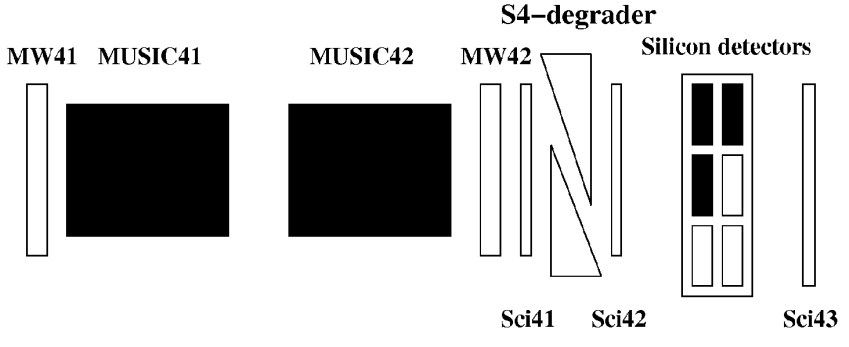

Fig. 1. Schematic of the detector configuration at the final focus of the GSI Fragment Separator for the current work. Note that only three of the possible six positions (black boxes) in the active stopper were occupied by DSSSDs in this particular experiment. MW = MultiWire position detectors; Sci=plastic scintillator detectors. The number "4" corresponds to the detectors being placed at the final focus, (i.e. after the 4th dipole magnet) GSI Fragments Separator. The secondary beam would be moving products from left to right on this schematic.

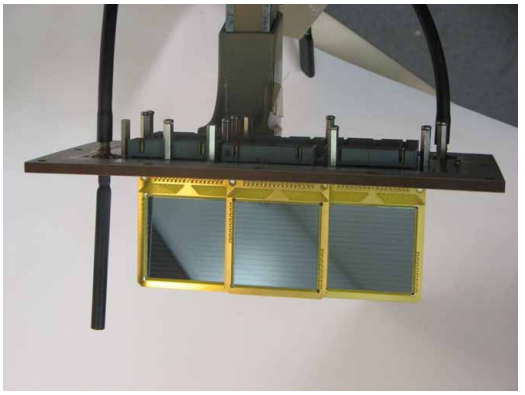

Fig. 2. Photograph of the bare DSSSDs used in the RISING active stopper in their holder with the light-tight outer box removed. (Note this was not the final geometry used for the three DSSSDs in the current work.)

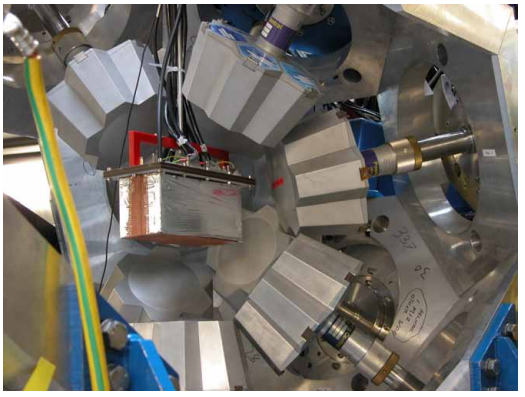

Fig. 3. Photograph of the DSSSDs in-situ at the centre of the RISING array in its Stopped Beam configuration. The active stopper is housed in the light tight box in the middle of the opened array.

and its daughter decays. The ultimate aim of the device is to correlate beta-decay events with specific exotic radioactive mother nuclei on an event-by-event basis. Figures 2 and 3 show photographs of the bare DSSSDs and their position within a light-tight box placed in the middle of the RISING array.

The technical difficulty with such measurements is that the dynamic range for the measurement of secondary reaction products and β-particles are orders-of-magnitude apart (i.e. $\sim$many GeV for the implanted fragment kinetic energies and $\sim$200 keV $\rightarrow$ a few MeV for the β-particles. This issue was addressed in the current work by the utilization of a pre-amplifier for the DSSSD energy signals, which was linear in the low-energy response range, followed by a logarithmic response at

higher gains. Semi-logarithmic preamplifiers were used, providing linear amplification up to 10 MeV and logarithmic amplification for the 10 MeV $\rightarrow$ 3 GeV range. The linear part allowed for both measurements of β (and in principle also, the spectroscopy of the charged particle decay) and was calibrated using an open, internal conversion electron ^{207}Bi source, yielding an energy resolution of FWHM = 20 keV and a minimum detection threshold of approximately 200 keV. The logarithmic part of the DSSSD output range allowed for the determination of the implantation position in an individual pixel (i.e. the pixel with maximum energy output compared to its neighbors) and was calibrated for energy response using a pulser. Scintillation detectors were placed both in front of and behind the catcher, allowing the off-line suppression of the majority of fragments which were destroyed in the slowing down process. Further details on the response of the semi-logarithmic pre-amplifier can be found in a forthcoming paper.[18]

3. Experimental Details, Data Analysis and Results

The experiment used to commission the RISING Active Stopper used a ^{208}Pb primary beam accelerated using the SIS-18 synchrotron at GSI to an energy of 1 GeV per nucleon and impinging on a 2.5 g/cm^2 thick Be target. The secondary products of interest were transmitted through the FRS and particle identification made on an event-by-event basis using the standard magnetic rigidity, time-of-flight, energy loss and position measurements (details of the particle identification procedure can be found in Refs. 5, 13, 19). A number of FRS settings were selected to maximize the transmission of a range of nuclei and the FRS was operated in achromatic mode in order to spread out the area of implantation of ions at the final focus thus reducing the ion-implantation rate per DSSSD pixel. This paper shows results from 2 settings, one centered on ^{188}Ta and the other on ^{190}Ta. Typical primary beam currents were 10^8 and 10^9 particles per beam spill for the ^{188}Ta and ^{190}Ta settings respectively. The typical beam spill length was approximately 1 second with a period of approximately 15 $\rightarrow$ 20 seconds.

3.1. *Particle identification procedure*

The nuclei of specific interest in this experiment were the neutron-rich Hf $\rightarrow$ Os nuclei with A$\sim$190. The study of heavy and exotic neutron-rich species can be hindered in such experiments by the presence of non-fully stripped ions (i.e., $Q \neq Z$) which are transmitted through the FRS in parallel with fully stripped ions. A prescription to (largely) eliminate this so-called $\frac{A}{Q}$ anomaly is outlined in Ref. 19 and uses the effective energy loss in the passive energy degrader placed at the central focus of the FRS to determine *changes* in charge state for ions as they pass through the first and second halves of the GSI fragment separator. Figure 4 shows the effect of plotting the energy loss of the ions as measured through a pair of Multi-Sampling Ionization Chambers (or "MUSIC") at the final focus of the FRS (see Fig. 1) versus the derived energy loss of the ions from their difference in magnetic rigidity through

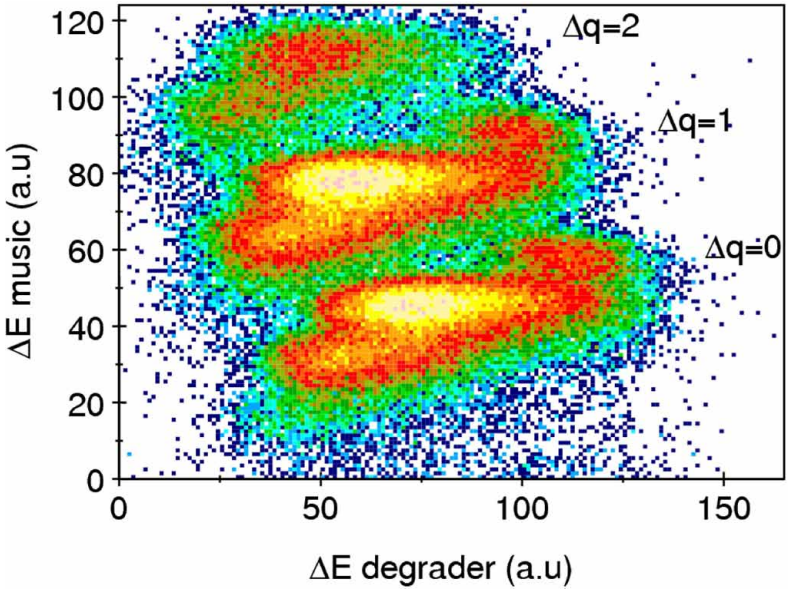

Fig. 4. Plot of ionic energy loss in the MUSIC detectors versus the derived energy loss in the passive degrader in the middle of the FRS for ions in the current experiment. Note the ions are separated into three distinct loci related to the *change* in charge state through the FRS. By far the most likely scenario for no change in charge state are those ions which are fully stripped (i.e. $Q = Z$) through both sections of the FRS.

the first and second halves of the FRS. This energy loss can be inferred from the measured time-of-flight of the ions in the second half of the FRS and the calculated time-of-flight of the ions in the first half of the separator.

Once the procedure outlined above had been applied to the events and (predominantly) fully-stripped ions with ionic charge, Q equal to Ze (where Z is the atomic number and e is the fundamental electronic charge) selected, a final, particle identification could be made for each ion on an event-by-event basis. This was made essentially using the measured time-of-flight of the ions as they passed through the second part of the FRS and known magnetic rigidity ($B\rho$) of the FRS dipole magnets, to calculate a value of mass over charge ($\frac{A}{Q=Z}$) for each ion. This quantity could then be correlated with the ion's energy loss (ΔE) as the ion passed through the MUSIC detectors, which is dependent on the atomic number Z. The responses of the detectors to specific values of $\frac{A}{Q}$ and Z for given velocities was determined following pre-experiment calibrations using the ^{208}Pb primary beam and could thus be applied to the final experimental data to provide calibrated measurements of the $\frac{A}{Q=Z}$ and Z values for each transmitted ion on an event-by-event basis by measuring their times-of-flight and energy losses respectively. Figure 5 shows a particle identification matrix from the current experimental work with a sum of two settings focussed on ions of ^{188}Ta and ^{190}Ta.

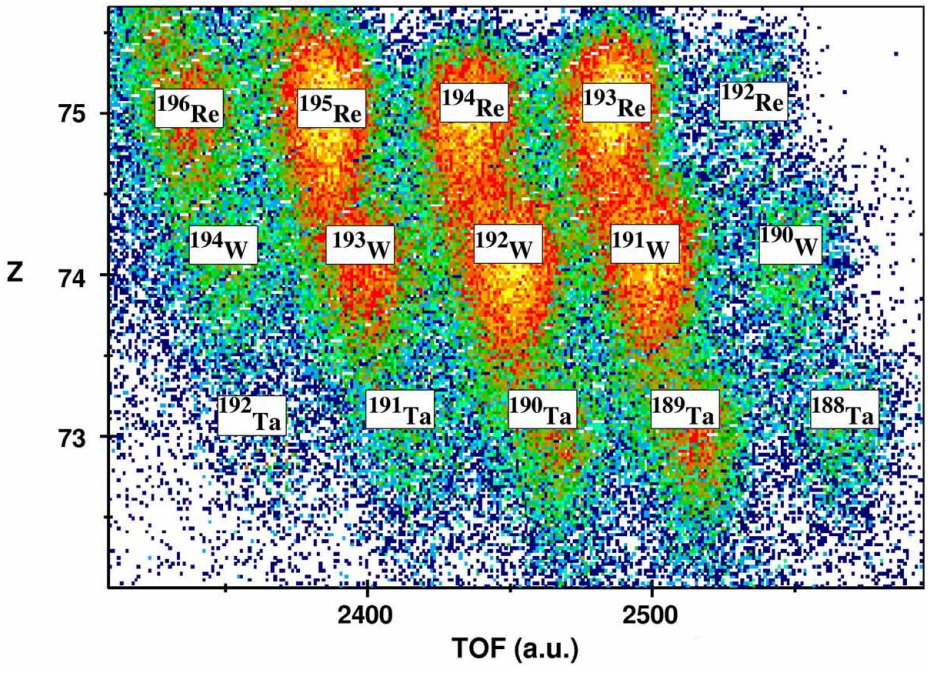

Fig. 5. Final particle identification plot for fully-stripped (i.e., $\Delta Q = 0$) ions following the fragmentation of a 1 GeV per nucleon ^{208}Pb beam. The data shown here are the sum of two FRS magnet settings centered on the transmission of ions of ^{188}Ta and ^{190}Ta respectively.

3.2. *Decays from isomeric states*

Decays from isomeric states in secondary beam particles which were transmitted through the FRS were observed in the RISING gamma-ray array. Since the gamma-ray transition energies and their decay lifetimes are characteristic of specific nuclei, these decays can be correlated with specific ions and used as an internal check and calibration of the particle identification procedure. Figure 6 shows gamma-ray spectra and their associated decay time profiles for previously reported[7] isomeric states in ^{188}Ta, ^{190}W and ^{192,193}Re which were observed in the current work. (Aside: We note in passing the apparent lack of evidence for the previously reported[4,7] 591 keV transition in the isomeric decay of ^{190}W. This is discussed further elsewhere[20,21]).

3.3. *Beta-delayed spectroscopy of secondary fragments*

Figure 7 shows the energy spectrum of ions and beta-particles taken from the sum of silicon strips in the three DSSSDs in the current work. Note that the use of the Mesytec 'semi-logarithmic' preamplifier allows the responses for both the heavy-ion implantation (i.e., the high energy *implant*) and beta-particle (low-energy *decay*) to be made using the same electronic channel. This allowed a clean identification pixel by pixel of the position of the implanted ion of interest which could then be

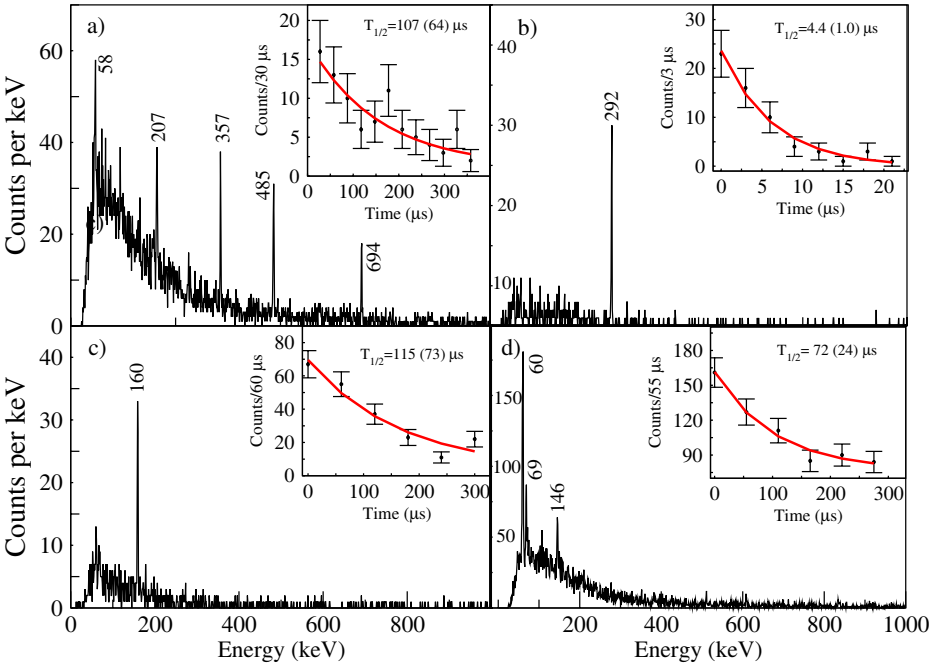

Fig. 6. Decays from previously reported[7] isomeric states in (a) ^{190}W, (b) ^{188}Ta, (c) ^{192}Re and (d) ^{193}Re observed in the current work and used to validate the particle identification procedure.

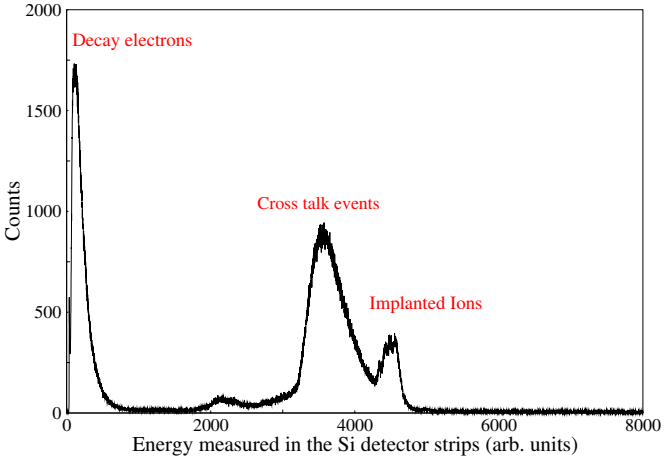

Fig. 7. Energy response spectrum (on a mixed linear and logarithmic scale) for the sum of each of the strips in the three DSSSDs used in the current work. The energy response of the detector is determined by the use of the Mesytec "semi-logarithmic pre-amplifier" which allows both β particles (energies ∼200 keV → a few MeV) and implanted secondary projectile fragments (energies ∼GeV to be measured in the same electronics channel. For more details see Ref. 18.

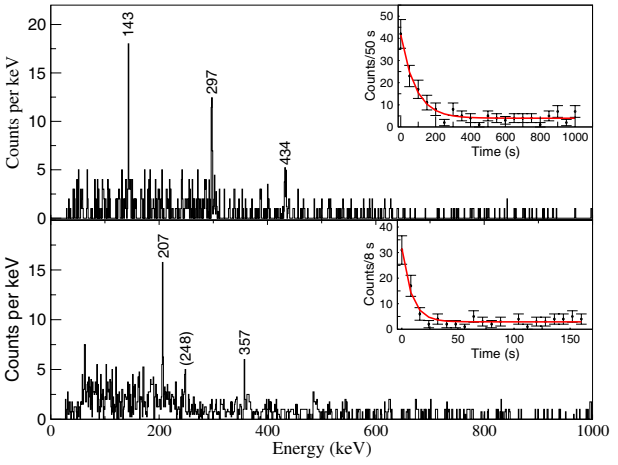

Fig. 8. Beta-delayed gamma-ray spectra from the current work showing transitions in ^{188}W and ^{190}W following the correlated β^- decay of ^{188}Ta and ^{190}Ta ions respectively. The insets show the measured time difference spectra between the radioactive tantalum implants and their subsequent β^- decays in the same or directly neighboring pixel in the DSSSDs.

correlated with subsequent β^- decay events (i.e., low-energy events measured in the DSSSDs) in the same and directly neighboring pixels. By investigating temporally-correlated $\beta^- - \gamma$ events with prompt gamma-ray coincidences between the β^- particle and γ rays measured in the Stopped RISING array, nuclide specific, β^--delayed gamma-ray spectra could be obtained providing spectral information on the daughter nuclei of the primary radioactive implants.

Figure 8 shows the gamma-ray spectra in coincidence with β^- particles following decays from the ^{188}Ta and ^{190}Ta mother nuclei (i.e., gamma-ray transitions in the daughter ^{188}W and ^{190}W respectively). The spectra showing the gamma rays correlated with the $^{188}\text{Ta} \rightarrow {}^{188}\text{W}$ decays clearly identify transitions at energies of 143, 297 and 434 keV respectively. These transitions have been previously reported as decays from the yrast states in ^{188}W with spin/parities of 2^+, 4^+ and 6^+ respectively as observed from in-beam studies using deep-inelastic[22] and two-neutron transfer reactions.[23] Transitions from states with spins greater than $6\hbar$ reported in Ref. 23 are not observed in the present work which is populated following β^- decay.

Similarly, the β^--correlated decays of transitions in ^{190}W in the current work show the previously reported[4,7] transitions at 207 and 357 keV. Note that the same transitions are also observed in the isomeric population of this nucleus in the current work (see Fig. 6(a)), however the 485 and 694 keV transitions identified in the isomeric decay are not observed in the β^--delayed feeding of this nucleus in the present work. On this basis and their relative intensities, the 207 and 357 keV transitions are thus established as the decays from the yrast 2^+ and 4^+ states in ^{190}W respectively.

4. Discussion of Preliminary Results

The energy systematics of the low-lying excited states in heavy nuclei can be used as a first insight into the structural properties of such nuclei. In cases such as the present work when the nuclei of interest are at the limits of experimental accessibility, it is often only the energy systematics which can be measured and used to obtain and extend global systematics of nuclear structure over long chains of proton and neutron number. Figure 9 shows the energy systematics of a wide chain of W and Os isotopes including the data from the current work on ^{190}W. Both the increasing energy of the yrast 2^+ energy and the parallel reduction in the energy ratio between the yrast 4^+ and 2^+ states is indicative of a reduction in collectivity as the neutron number of these elements approaches the N=126 closed shell.

The ratio of the 4^+ to 2^+ energies in ^{190}W has been the subject of some discussion in the literature with Os and W nuclei around A$\sim$190 $\rightarrow$ 194 being proposed as possible candidates for weakly-deformed *oblate* shapes.[4,24–27] Possible evidence for such a sudden change from well-deformed, prolate ground-state shapes to weakly-deformed oblate shapes might be evidenced by discontinuities in the energy systematics of such nuclei. Such spectral information can be obtained using the β^--delayed spectroscopic technique outlined above.

Figure 10 shows Hartree–Fock calculations assuming axial symmetry for neutron-rich W and Os nuclei around A$\sim$190. The prolate-oblate minima are pre-

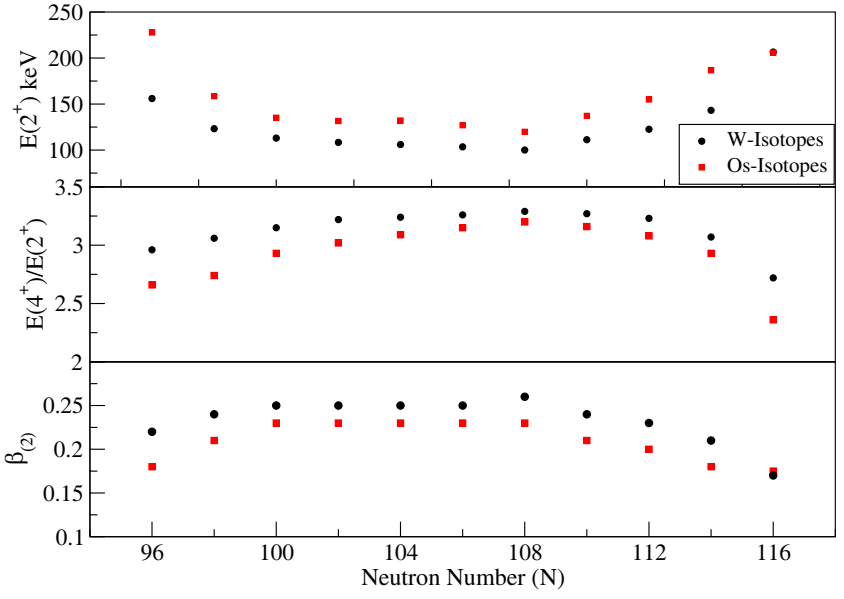

Fig. 9. Low-lying energy systematics of even-even W and Os isotopes, including data from the current work. The deformation parameter, β_2 is inferred from the empirical relation proposed by Raman.[28]

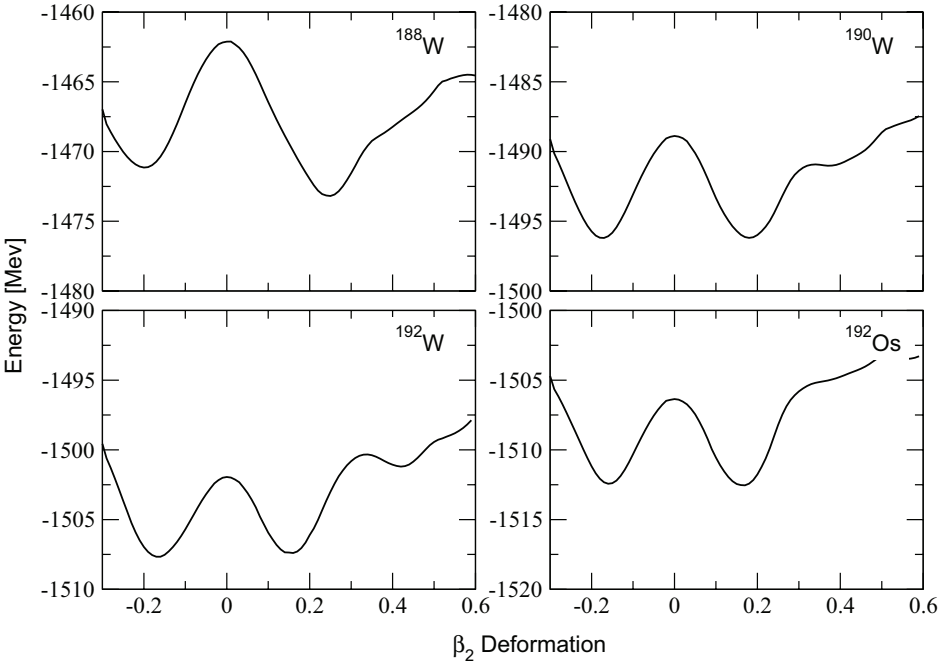

Fig. 10. Hartree–Fock calculations (assuming axially symmetry) of the ground state energy of ^{188,190,192}W and ^{192}Os a function of quadrupole deformation, β_2. For more details, see Ref. 24.

dicted to be competitive in this region with them being almost equal in energy for ^{190}W with the calculations suggesting that the oblate minimum becomes favored for the N = 118 isotone ^{192}W. The estimate for the quadrupole deformation, β_2, inferred from the empirically derived relation with the energy of the first 2^+ state by Raman *et al.*,[28] is consistent with the magnitude of the deformation predicted for the preferred minimum in the calculations shown in Fig. 10.

5. Summary and Future Work

In summary, the RISING active stopper has been used for gamma-ray spectroscopic measurements following the correlated beta-decays of heavy neutron-rich nuclei in the Hf → Os region for the first time. The measurements demonstrate the power of the decay spectroscopy techniques when applied to the projectile fragmentation mechanism for the production and selection of nuclear species with very exotic proton-to-neutron ratios. The first data allowing correlated gamma-ray spectroscopic measurements following the beta-decay of the neutron-rich ^{188,190}Ta isotopes into their W daughter nuclei highlights the effectiveness of the RISING "Active stopper" in such studies. Similar measurements have been made from the same data set on previously reported[29,30] decays from ^{192}Re and ^{198}Ir and the

current data have also been used to establish the beta-decay of ^{194}Re for the first time,[31] with the expected gamma-ray transitions in the ^{194}Os daughter nucleus[32] have been clearly identified. The spin/parities populated in the daughter nuclei can then be used with the measured lifetime of the decay to deduce the $F\tau$ value for that particular β^- decay. This can be used with the standard β^- decay selection rules to infer the spin/parity of the mother nucleus which can also be used to infer information on the shape (i.e. prolate or oblate) of the mother nucleus.[33]

The active stopper can also be used to measure decays from long-lived ($T_{\frac{1}{2}}$ ∼seconds) states which decay with significant internal conversion branches. Discrete-line internal conversion energy data have been observed in the same experiment[34] discussed in this paper from the internal decay between the proposed $\frac{11}{2}^-$ and $\frac{3}{2}^+$ states in the N = 126 isotone ^{205}Au with the particle identification of this nucleus confirmed using the observation of the previously reported[35] γ rays observed in the daughter nucleus following the β^- decay of the ^{205}Au ground state. Other subsequent measurements using the active stopper for beta-delayed measurements of fragmentation products of ^{238}U primary beams have also been carried out. Together with the present work this technique expands the regime of nuclei available for spectral study and is of particular significance for heavy neutron-rich nuclei approaching the rapid-neutron process paths around N∼126.

References

1. A. Gade and T. Glasmacher *Prog. Part. Nucl. Phys.* **60** (2008) 161; R. F. Casten and B. M. Sherrill *Prog. Part. Nucl. Phys.* **45** (2000) S171.
2. H. Geissel, *Nucl. Instr. Meth. Phys. Res. B* **261** (2007) 1079.
3. M. Pfützner *et al.*, *Phys. Lett. B* **444** (1998) 32.
4. Zs. Podolyák *et al.*, *Phys. Lett. B* **491** (2000) 225.
5. M. Pfützner *et al.*, *Phys. Rev. C* **65** (2002) 064604.
6. Zs. Podolyák *et al.*, *Nucl. Phys. Phys. A* **722** (2003) 273c.
7. M. Caamano *et al.*, *Eur. Phys. J. A* **23** (2005) 201.
8. K. A. Gladnishki *et al.*, *Phys. Rev. C* **69** (2004) 024617
9. Zs. Podolyák *et al.*, *Phys. Lett. B* **632** (2006) 203.
10. P. H. Regan *et al.*, *Nucl. Phys. A* **787** (2007) 491c.
11. A. Jungclaus *et al.*, *Phys. Rev. Lett.* **99** (2007) 132501.
12. A. B. Garnsworthy Ph.D. Thesis, Univ. of Surrey, UK (2007).
13. A. B. Garnsworthy *et al.*, *Phys. Lett. B* **660** (2008) 326.
14. M. Górska *et al.*, *Acta. Phys. Pol. B* **28** (2007) 1219.
15. H. J. Wollersheim *et al.*, *Nucl. Inst. Meth. Phys. Res. A* **537** (2005) 637.
16. S. Pietri *et al.*, *Acta Phys. Pol. B* **38** (2007) 1255.
17. S. Pietri *et al.*, *Nucl. Inst. Meth. Phys. Res. B* **261** (2007) 1079.
18. R. Kumar *et al.*, *submitted to Nucl. Inst. Meth. Phys. Res. A.*
19. J. Benlliure *et al.*, *Nucl. Phys. A* **660** (1997) 87; erratum *Nucl. Phys. A* **674** (2000) 578.
20. G. Farrelly, Zs. Podolyák *et al.*, private communication.
21. G. J. Lane *et al.*, contribution to the Nuclear Structure NS08 Conference, Michigan State University (2008).
22. Zs. Podolyak *et al.*, *Int. J. Mod. Phys. E* **13** (2004) 123.

23. T. Shizuma *et al.*, *Eur. Phys. J. A* **30** (2006) 391.
24. P. D. Stevenson *et al.*, *Phys. Rev. C* **72** (2005) 047303.
25. P. Finelli *et al.*, *Nucl. Phys. A* **770** (2006) 1.
26. P. Sarriguren *et al.*, *Phys. Rev. C* **77** (2008) 064322.
27. J. Jolie and A. Linnemann *Phys. Rev. C* **68** (2003) 031301.
28. S. Raman *et al.*, *At. Data Nucl. Data Tables* **78** (2001) 1.
29. C. M. Baglin *Nuc. Data Sheets* **84** (1998) 717.
30. Z. Chunmei, *Nucl. Data. Sheets* **95** (2002) 59; A. Szalay and S. Uray, *Radiochim. Radioanal. Lett.* **14** (1973) 135.
31. P. H. Regan and N. Al-Dahan *et al.*, in the Proceedings of the 13th Conference on Capture Gamma Spectrosocopy and Related Topics, Köln, Germany (2008), to be published in AIP Conference Proceedings.
32. C. Wheldon *et al.*, *Phys. Rev. C* **63** (2001) 011304.
33. P. M. Walker and F. R. Xu *Phys. Rev. C* **74** (2006) 067303.
34. Zs. Podolyák, G. Farrelly and P. H. Regan *et al.*, *submitted to Phys. Lett. B.*
35. F. G. Kondev *Nucl. Data Sheets* **101** (2004) 521; Ch. Wennemann *et al.*, *Z. Phys. A* **347** (1994) 185.